Insights into lithospheric architecture, fertilisation and fluid pathways from AusLAMP MT

Stephan Thiel*
Department of State Development
Geological Survey of South Australia
Level 4, 101 Grenfell Street
Adelaide, SA 5000
Geology and Geophysics
School of Physical Sciences
The University of Adelaide
Adelaide, SA 5005
stephan.thiel@sa.gov.au

Graham Heinson
Geology and Geophysics
School of Physical Sciences
The University of Adelaide
Adelaide, SA 5005

Anthony Reid
Department of State Development
Geological Survey of South Australia
Level 4, 101 Grenfell Street
Adelaide, SA 5000

Kate Robertson
Geology and Geophysics
School of Physical Sciences
The University of Adelaide
Adelaide, SA 5005

**presenting author asterisked*

SUMMARY

The Australian Lithospheric Architecture Magnetotelluric Project (AusLAMP) has the goal to map the electrical resistivity of the Australian lithosphere to constrain the geodynamic framework of the continent. Data acquisition in South Australia has covered two-thirds of the state to date. Three-dimensional resistivity models of subsets of the AusLAMP grid across the Gawler Craton show a generally electrically resistive crust and lithosphere, but an area of low resistivity between depths of 100 km and 200 km beneath the Gawler Range Volcanics exists. A possible explanation is a fertilised mantle signature as a result of metasomatic events in the Proterozoic. The continuous low resistivity connection along the margins of the Gawler Craton core to the surface coincides with the prospective IOCG belt along the eastern margin of the Gawler Craton. The results support the importance of the AusLAMP project to define the lithospheric architecture of the continent and the value of primary lithospheric architecture for mineral exploration.

Key words: magnetotellurics, lithosphere, AusLAMP, South Australia, Gawler Craton

INTRODUCTION

Exploration under cover remains one of the main impediments to mineral exploration in Australia. With a lack of conclusive mineral pointers from upper crustal and near-surface geophysical techniques, such as potential field methods, the push to understanding mineral systems across the entire lithospheric column provides a promising addition to mineral exploration packages. Additionally, the constraints on lithospheric architecture and insights into composition shed a crucial light on the tectonic setting mineral fertility corridors. With an increased understanding of a whole lithosphere approach to exploration (Griffin et al., 2013), deep probing geophysical techniques such as magnetotellurics (MT) (Heinson et al., 2006; Thiel and Heinson, 2010; Thiel and Heinson, 2013) seismic tomography (Rawlinson et al., 2014) as well as geochemical sampling of the sub-continental lithospheric mantle (SCLM) (O'Reilly and Griffin, 2010) will play an increasingly important role in terrane-to-province selection of target areas for mineral exploration.

The illumination of crustal and SCLM using geophysical techniques is largely restricted to seismic and magnetotelluric techniques. The flexibility of MT for craton-wide deployments to close-spaced high resolution surveys across mineral deposits highlights the technique's ability to image across all scales from depths of a few tens of metres to hundreds of kilometres. The sensitivity of MT to electrical resistivity stresses its importance in detection of usually minor conducting phases such as fluids and fluid precipitates (graphite, sulphide, mineralisation). Fluid pathways are often connected to structural boundaries characterised by changes in rheology, associated with gradients in density, magnetic susceptibility and elastic properties.

The Australian Lithospheric Architecture Magnetotelluric Project (AusLAMP) uses long-period (5-20,000 s) (MT) data spaced every half degree latitude and longitude to map the electrical resistivity of the crust and mantle lithosphere. The project is designed to improve the understanding of the lithosphere as a primary control for mineral deposits. It is widely accepted that varying lithospheric strength plays a key role in localisation of deformation and channelling of magmatism and fluid flow in the crust and mantle.

The AusLAMP South Australia program, funded in various stages by the Geological Survey of South Australia (GSSA), and University of Adelaide (UofA) and Geoscience Australia (GA) has deployed over 200 long-period (5 s to 10 000 s) MT sites across South Australia south of 28° latitude from the border with Western Australia to New South Wales and Victoria in the east.

We report on a 3D resistivity model of the lithosphere beneath the Gawler Craton, South Australia, derived from over 150 AusLAMP MT stations, a subset of the current AusLAMP SA project.

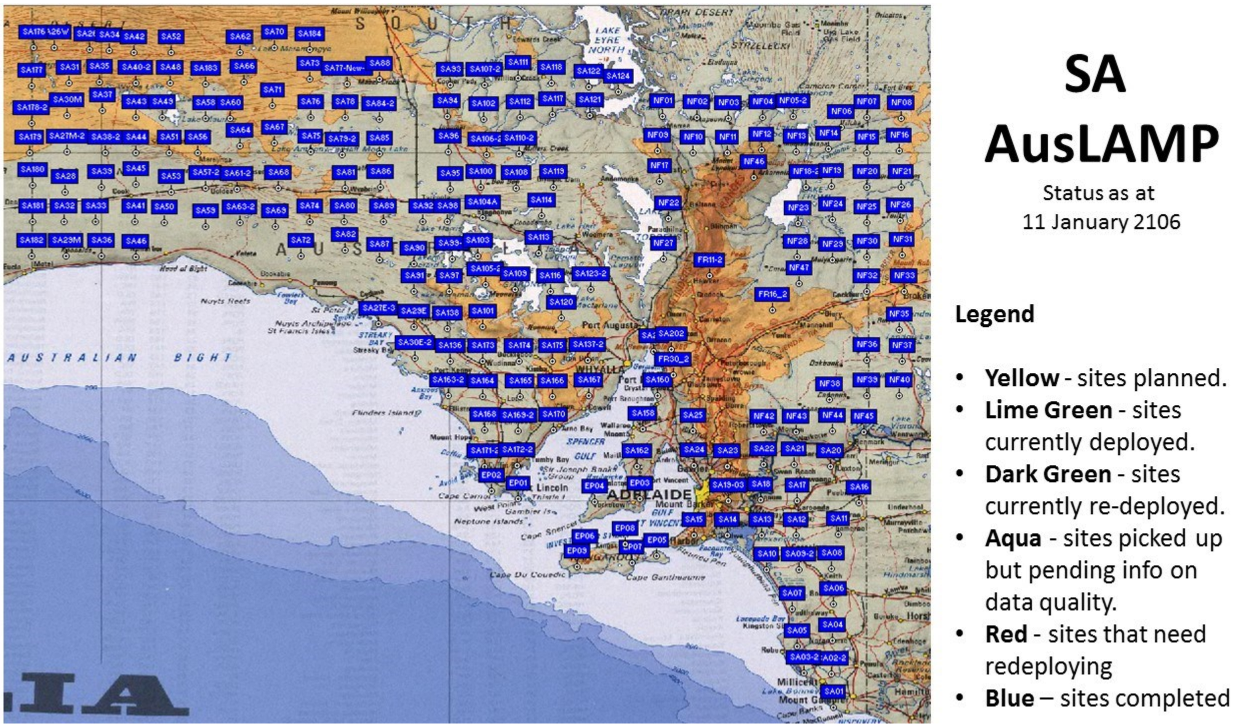

Figure 1: Coverage of long-period (10-10,000 s period) MT station of the AusLAMP SA project at January 2016. MT stations are placed every 0.5° latitude and longitude, ~55 km. Gaps in the grid have existing legacy MT data from previous surveys that meet the quality requirements of the AusLAMP grid. The models presented here are from MT data in the central part of the grid across the Gawler Craton, collected by The University of Adelaide (UofA) and the Geological Survey of South Australia (GSSA). Processing is underway for MT data in the west across the Maralinga Lands from a joint project between GSSA, Geoscience Australia (GA), and UofA).

METHOD AND RESULTS

Method

Magnetotellurics is a passive electromagnetic technique measuring natural variations of the Earth's magnetic and electric at the surface of the Earth (Cagniard, 1953). Interactions between the solar plasma with the Earth's ionosphere and magnetosphere (Frequency f< 10 Hz or its inverse period T>10 s) or global lightning activity (f>10 Hz) cause magnetic field variations, which act as a source for the induction of electric eddy currents in the Earth.

In the field, the MT systems sample time series of the horizontal electric field $\{E_x, E_y\}$ and the three-component magnetic field $\{B_x, B_y, B_z\}$, with $\{x, y,, z\}$ denoting geographic north, east, and vertically down, respectively. The time series convert into the frequency domain using robust remote referencing processing schemes (Chave and Jones, 2012; Chave and Thomson, 2004). The frequency of the signal as well as the bulk resistivity of the subsurface determines the penetration depth δ of the signal via the skin-depth relationship (in m):

$$\delta = 503\sqrt{\rho \cdot T}$$

The complex ratio of the horizontal electric to magnetic field, as a function of period T, yields the impedance tensor Z via:

$$[E_x \quad E_y] = \begin{bmatrix} Z_{xx} & Z_{xy} \\ Z_{yx} & Z_{yy} \end{bmatrix} \cdot \begin{bmatrix} B_x \\ B_y \end{bmatrix}$$

Each component of $Z = X + iY$ can be expressed as a magnitude ρ_a and phase ϕ as follows:

$$\rho_a = \frac{1}{\omega\mu_0} \left|Z_{ij}\right|^2$$

Where ω denotes the angular frequency, and μ_0 the magnetic permeability.

$$\phi = \tan^{-1}\frac{\Im Z_{ij}}{\Re Z_{ij}}$$

Where I and R denote the imaginary and real part of Z_{ij}, respectively. An alternative way to represent the impedance tensor information is the galvanic distortion free magnetotelluric phase tensor.

$$\Phi = X^{-1}Y$$

Its representation as an ellipse readily shows the dimensionality and strike of the impedance tensor. One-dimensional resistivity distributions are characterized by a circle. Ellipses denote 2D or 3D structure, with a non-zero value of the phase tensor skew $\beta = \frac{1}{2}\tan^{-1}\frac{\phi_{12} - \Phi_{21}}{\phi_{11} + \Phi_{22}}$ pointing to 3D structures. The principal components of the phase tensor denote the transverse electric and transverse magnetic polarization phases in 2D and are therefore parallel or perpendicular to the geoelectric strike.

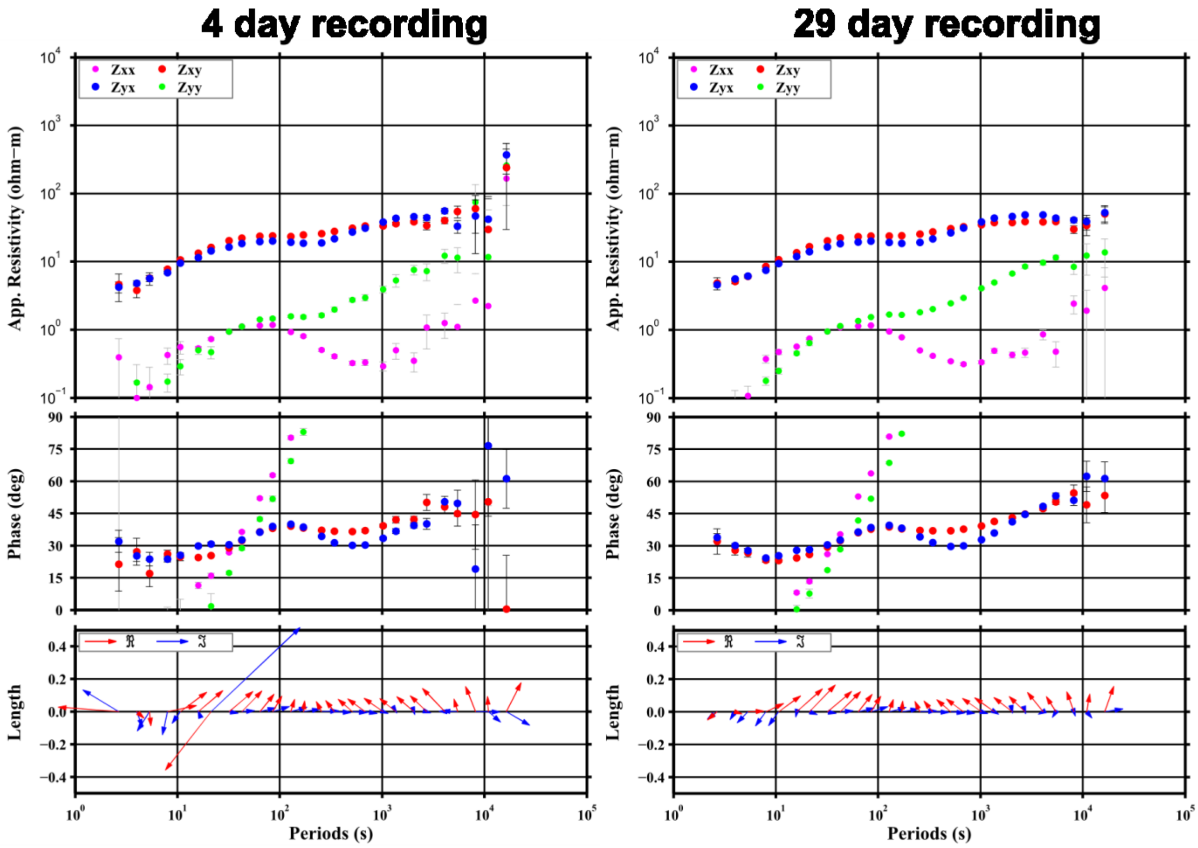

Figure 2: Apparent resistivity, phase and tipper (top to bottom) curve for station SA111 in the north-eastern part of the grid. The long deployment time of 3-4 weeks (right) compared to previously recorded long-period MT data across the state (left, same site) illustrates the improvement in data quality, especially at long periods penetrating mantle depths.

Results

The MT data is generally of very good quality with smooth impedance and tipper responses between 5 s and over 10,000 s (Figure 2). Apparent resistivities are higher on average across the entire frequency range for stations across the central part of the Gawler Craton, exceeding 1000 Ωm. Figure 2 shows a typical response for a station along the margins of the craton, with lower resistivities of few tens of Ωm across the frequency band. The induction arrows, a representation of the ratio between the anomalous vertical magnetic field, due to subsurface structure, and the horizontal magnetic field, further supports the first order resistive nature of the Gawler Craton compared to its margins (Figure 3). Induction arrows at a period of 1000 s have a larger magnitude with a predominant orientation towards the semi-circular margin of the craton signifying the resistivity contrast from resistive to the more conductive margin.

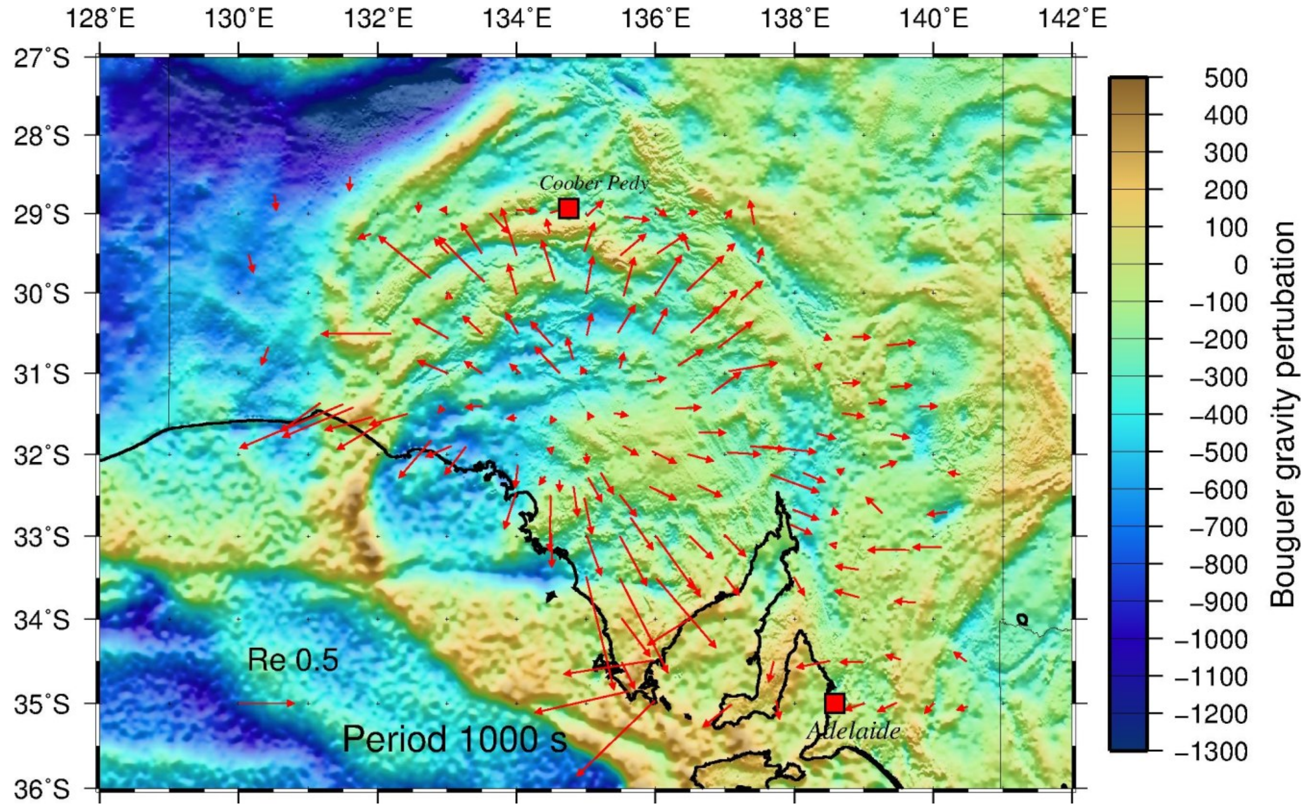

Figure 3: Induction arrows for period of 1000 s of the data used in the 3D inversion.

The impedances for 22 periods between 10 s and 16000 s of 156 stations were inverted using a 3D non-linear conjugate gradient smooth inversion code ModEM (Egbert and Kelbert, 2012; Kelbert et al., 2014). Tests with varying inversion parameters such as the trade-off between model smoothness and data fit, as well as a-priori constraints such as the inclusion of sea water show that results are robust. A final nRMS of 1.85 was achieved for the model shown in Figure 4.

Areas of low mantle resistivity (<10 Ωm) at depths greater than 100 km beneath the Gawler Range Volcanics suggest widespread fertilisation of the inferred Archean-Proterozoic lithospheric core of the Gawler Craton. The lithosphere-asthenosphere boundary (LAB) beneath the Gawler Craton, derived from p- and S-wave arrivals, is on the order of ~200 km. A reduction in resistivity due to asthenosphere melts is not expected and temperatures are not high enough for partial melts to occur. Instead a minor conductive phase in nominally anhydrous mantle rocks is the likely cause for a decrease in resistivity. A connection of the low resistivity region to the surface occurs around the eastern margin of the Gawler Craton, a region with extensive magmatism and Cu-Au mineralisation, particularly at Olympic Dam. Indeed, the conductivity anomaly suggests a causal link between mantle fertilisation and mineral enrichment in the crust.

In contrast, beneath the south-western region of the craton the electrical resistivity is high (>1000 Ωm) to depths exceeding 200 km. If the inferred mantle fertility beneath the central-eastern Gawler Craton is due to metasomatic input from an Archean or Proterozoic subduction setting, it did not have a pervasive effect on the SCLM of the western part of the craton.

The broad-scale pattern of the SCLM electrical resistivity seen in the AusLAMP data is matched by the more evolved εNd isotopic values of syn-mineralisation (c. 1.59 Ga) magmatism around the margins of the craton.

CONCLUSIONS

The 3D inverse model of the Gawler Craton shows for the first time a detailed image of the mantle and crustal lithosphere of the resistivity distribution beneath the Gawler Craton. The prospective IOCG belt along the eastern margin of the craton is electrically conductive and is connected to a mantle conductivity anomaly at depths between 100 km and 200 km. Taken together, these data support a hypothesis that links: (i) magmatism derived from a metasomatically enriched, and therefore more evolved mantle, (ii) large-scale crustal contamination of syn-mineralisation mantle melt, and (iii) large-scale regional fluid pathways revealed in the 3D MT data to the Cu-Au mineralisation prevalent along the eastern margin of the craton. In addition, the IOCG prospects across the Yorke Peninsula and the Stuart Shelf appear not connected in the mid to lower crust.

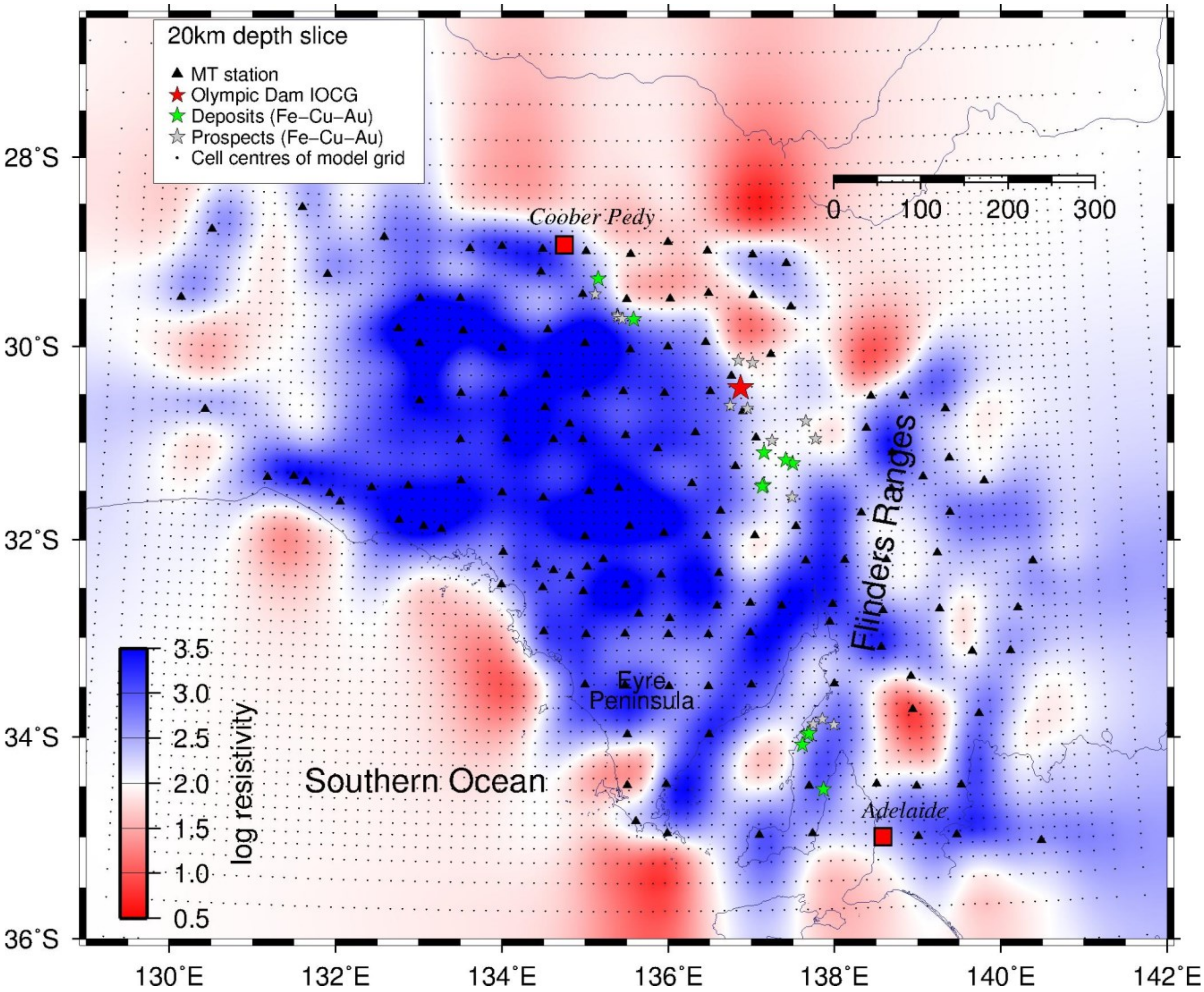

Figure 4: Resistivity slice at 20 km depth derived from 3D inversion of impedances for 22 periods between 10 s and 16000 s of 156 MT stations (black triangles). Model grid nodes are shown as small black dots. The model is best constrained beneath locations of MT stations.

ACKNOWLEDGMENTS

Philippa Mawby, Geoff Axford and Bruce Goleby and numerous PhD students of University of Adelaide are thanked for field work. Ian Hopton (DSD) and AARD helped with Aboriginal liaison. David Love (DSD) provided help with land access. We thank pastoralists, Indigenous land owners, WPA personnel and National Parks SA for access to land. Data was collected using the AuScope National MT instrument pool. Geoscience Australia is thanked for discussions and support of the AusLAMP initiative.

REFERENCES

Cagniard, L., 1953. Basic theory of the magneto-telluric method of geophysical prospecting. Geophysics, 18: 605-635.

Chave, A.D. and Jones, A.G., 2012. The Magnetotelluric Method: Theory and Practice. Cambridge University Press.

Chave, A.D. and Thomson, D.J., 2004. Bounded influence magnetotelluric response function estimation. Geophysical Journal International, 157(3): 988-1006.

Egbert, G.D. and Kelbert, A., 2012. Computational recipes for electromagnetic inverse problems. Geophysical Journal International, 189(1): 251-267.

Griffin, W.L., Begg, G.C. and O'Reilly, S.Y., 2013. Continental-root control on the genesis of magmatic ore deposits. Nature Geoscience, 6: 905-910.

Heinson, G.S., Direen, N.G. and Gill, R.M., 2006. Magnetotelluric evidence for a deep-crustal mineralizing system beneath the Olympic Dam iron oxide copper-gold deposit, southern Australia. Geology, 34: 573-576.

Kelbert, A., Meqbel, N., Egbert, G.D. and Tandon, K., 2014. ModEM: A modular system for inversion of electromagnetic geophysical data. Computers & Geosciences, 66(0): 40-53.

O'Reilly, S.Y. and Griffin, W.L., 2010. The continental lithosphere-asthenosphere boundary: Can we sample it? Lithos, 120(1-2): 1-13.

Rawlinson, N., Salmon, M. and Kennett, B.L.N., 2014. Transportable seismic array tomography in southeast Australia: Illuminating the transition from Proterozoic to Phanerozoic lithosphere. Lithos, 189(0): 65-76.

Thiel, S. and Heinson, G., 2010. Crustal imaging of a mobile belt using magnetotellurics: An example of the Fowler Domain in South Australia. Journal of Geophysical Research, 115(B6): B06102-B06102.

Thiel, S. and Heinson, G., 2013. Electrical conductors in Archean mantle - result of plume interaction? Geophysical Research Letters, 40: 2947-2952.